

Zero bias conductance peak in InAs nanowire coupled to superconducting electrodes

Nam-Hee Kim^{1,§}, Yun-Sok Shin^{2,§}, Hong-Seok Kim¹, Jin-Dong Song³, Yong-Joo Doh^{1*}

¹Department of Physics and Photon Science, Gwangju Institute of Science and Technology, Gwangju 61005, Republic of Korea

²Sejong Academy of Science and Arts, Sejong 30099, Republic of Korea

³Korea Institute of Science and Technology, Seoul 02792, Republic of Korea

*E-mail: yjdoh@gist.ac.kr

§These authors contributed equally to this work.

Abstract

We report the occurrence of the zero-bias conductance peak (ZBCP) in an InAs nanowire coupled to PbIn superconductors with varying temperature, bias voltage, and magnetic field. The ZBCP is suppressed with increasing temperature and bias voltage above the Thouless energy of the nanowire. Applying a magnetic field also diminishes the ZBCP when the resultant magnetic flux reaches the magnetic flux quantum $h/2e$. Our observations are consistent with theoretical expectations of reflectionless tunneling, in which the phase coherence between an electron and its Andreev-reflected hole induces the ZBCP as long as time-reversal symmetry is preserved.

Keywords: zero-bias conductance peak; InAs nanowire; Andreev reflection; reflectionless tunneling

Nano-hybrid superconducting devices, which consist of low-dimensional nanostructures in contact with superconducting electrodes, provide a useful platform for developing novel quantum information devices. In particular, InAs nanowires (NWs) have attracted intense interests as a good material system for fabricating nano-hybrid superconducting devices owing to their outstanding electrical properties, such as high electron mobility, low effective mass, and relatively easy formation of low ohmic contacts. So far, a supercurrent transistor [1], NW quantum dot [2], quantum electron pump [3], Cooper pair splitter [4], and gate tunable superconducting qubit [5, 6] have been developed with InAs NWs. As a signature of a Majorana fermion, which is a particle identical to its own antiparticle, the zero-bias conductance peak (ZBCP) has also been observed in an InAs NW coupled to a superconducting electrode [7]. Because the ZBCP can also be caused by reflectionless tunneling [8] due to an incomplete superconducting proximity effect, more extensive studies are required to verify the physical origin of the ZBCP observed in InAs NWs.

The superconducting proximity effect in nano-hybrid superconducting junctions can be understood with the Andreev reflection [9], where an electron incident upon the interface between a normal metal (N) and superconductor (S) can be retro-reflected into the N region as a phase-conjugated hole while leaving a Cooper pair in the S region. As a result, the Andreev reflection occurring at an ideal N–S interface results in a twofold increase of the conductance for bias voltages smaller than Δ/e , where Δ is the superconducting energy gap. With a non-ideal N–S interface, there exists a finite probability for the incident electron to be partially reflected as an electron and also retro-reflected as a hole via the Andreev reflection. When the mirror-reflected electron undergoes several scatterings with disorder centers in the N region and is incident on the N–S interface again, an additional Andreev reflection can occur. This results in another retro-reflected hole tracing back the previous scattering paths

and continuing successive Andreev reflections. This process, which is called reflectionless tunneling [8], can also cause a ZBCP in a sample including the N–S interface. So far, the ZBCP due to reflectionless tunneling has been observed in several nano-hybrid superconducting junctions made of graphene [10] and InAs NW [11]. However, the observed values of the characteristic voltage and temperature for the ZBCP are not consistent with the theory [8], which has been attributed to a degradation effect at the N–S interface reducing the diffusion constant [11]. Here, we report the observation of a ZBCP obtained from an InAs NW in contact with superconducting PbIn electrodes. Our extensive studies of ZBCPs with a varying bias voltage, temperature, and magnetic field revealed that our observed ZBCP is due to the phase-coherent quantum electronic transport, which is consistent with the reflection tunneling theory.

InAs NWs were grown on a Si substrate by ultrahigh vacuum molecular beam epitaxy with gold particles (~50 nm diameter) as the catalyst [12]. The as-grown InAs NWs were transferred to a highly *p*-doped Si substrate covered by a 300 nm thick oxide layer. Source and drain electrodes were patterned by conventional *e*-beam lithography, followed by *e*-beam evaporation of 170 nm thick PbIn film. Prior to the metal deposition, the NW surface was cleaned with an Ar ion beam to remove a presumed native oxide layer. The PbIn alloy source was made by using a mixture of lead (Pb) and indium (In) pellets with a weight ratio of 9:1. The 10 nm thick Au film was used as a capping layer. Figure 1a shows a scanning electron microscopy (SEM) image of sample **D1** after the device fabrication process was completed. The superconducting transition temperature and perpendicular critical field of the PbIn film were obtained as $T_C = 7.3$ K and $B_C = 0.24$ T, respectively [13]. The differential resistance dI/dV was measured by using a standard lock-in technique of superimposing a small AC signal with a frequency of 37.77 Hz onto the DC bias current. For low-noise measurement,

two-stage resistor–capacitor (RC) filters (cutoff frequency = 10 kHz) and π filters were connected in series to the measurement leads [14].

Figure 1b displays the conductance G of sample **D2** as a function of the backgate voltage V_g at $T = 10$ K. This indicates n -type conduction of the InAs NW. The electron mobility was $\mu = dG/dV_g \times L^2/C_g = 3800$ cm²/Vs, where L is the channel length and C_g is the gate capacitance between InAs NW and the Si substrate [15]. The diameter and channel length of sample **D1** were $d = 80$ nm and $L = 220$ nm, respectively. Those for sample **D2** were $d = 60$ nm and $L = 590$ nm, respectively. For sample **D2**, the carrier density is about $n \sim 2.8 \times 10^{17}$ cm⁻³ and the mean free path is $l_m = 41$ nm at $V_g = 0$ V.

When the temperature was lowered below T_C , the sample resistance started to increase and display an insulating $R(T)$ behavior (see Figure 2a). At lower temperatures near $T^* = 3.6$ K, the insulating behavior changed to the metallic one. The former insulating $R(T)$ curve near T_C can be understood with the Blonder–Tinkham–Klapwijk (BTK) theory, which considers the interfacial barrier effect at the N–S contact. According to BTK theory, the current flowing through the N–S interface is given by [16]

$$I_{NS} = \frac{1+Z^2}{eR_N} \int_{-\infty}^{\infty} [f_0(E - eV) - f_0(E)] \times [1 + A(E) - B(E)] dE, \quad (1)$$

where Z is a parameter characterizing the height of a presumable tunnel barrier at the N–S interface ($Z = 0$ for ideal transparency), V is the bias voltage, R_N is the normal-state resistance, f_0 is the Fermi–Dirac distribution function, $A(E)$ is the probability of the Andreev reflection, and $B(E)$ is the probability of the specular reflection. For $E < \Delta$, $A(E)$ is given by $\Delta^2/[E^2 + (\Delta^2 - E^2)(1 + 2Z^2)^2]$, and $B(E)$ is $1 - A(E)$. The $R(T)$ curve near T_C fitted well with the calculation result of $(dI_{NS}/dV)^{-1}$ using $Z = 2$ and $\Delta_0 = 1.14$ meV as fitting parameters, as shown in Figure 2a. Here, Δ_0 is a superconducting gap energy of the PbIn electrode at zero temperature. The

deviation between the calculation and experimental data occurring at lower temperatures is discussed later.

The differential conductance $G = dI/dV$ was plotted as a function of V at the base temperature $T = 2.4$ K (see Figure 2b). The $G(V)$ curve exhibited a ZBCP and additional peak structure at $V_{\text{gap}} = 2.3$ meV. The overall suppression of G below V_{gap} was attributed to the formation of a non-ideal N–S interface, and the dI/dV peak position on the V axis corresponds to the superconducting gap voltage Δ/e . Because there existed two N–S interfaces coupled in series via the InAs NW, the V_{gap} value resulted in $\Delta_{\text{PbIn}}(2.4 \text{ K}) = 1.15$ meV, where Δ_{PbIn} is the superconducting gap energy of PbIn electrodes. This result is consistent with the fitting result of $R(T)$ curve and other reports [14, 17].

We note that the ZBCP diminished at a characteristic voltage of $V^* = 0.22$ mV. Increasing the lock-in bias voltage showed a similar suppression of the ZBCP, as shown in Figure 2c. Because reflectionless tunneling arises from the quantum phase conjugation between the incident electron and Andreev-reflected hole, which traces back the path of the scattered electron, the characteristic voltage V^* for observing the ZBCP can be related to the Thouless energy $E_{\text{Th}} = eV^* = 0.22$ meV of the InAs NW. Then, the phase coherence time is given by $\tau_\phi = \hbar/E_{\text{Th}} = 3.0$ ps, which results in the phase-coherence length of $L_\phi = \sqrt{D\tau_\phi} = 205$ nm, where $\hbar = h/2\pi$ is the reduced Planck's constant, $D = v_F l_m/3 = 140$ cm²/s is the diffusion coefficient, and $v_F = 1.04 \times 10^6$ m/s is the Fermi velocity [18]. Because L_ϕ is close to the channel length $L = 220$ nm, we concluded that the whole NW segment between two PbIn electrodes contributes to the phase-coherent reflection tunneling to result in the observed ZBCP feature.

As we increased the temperature, the ZBCP height gradually decreased and

disappeared at the characteristic temperature $T^* = 3.6$ K, as shown in Figure 2d. This temperature-dependent behavior of the ZBCP is consistent with the metallic $R(T)$ curve below T^* in Figure 2a. Because the thermal coherence length [19] is given by $\xi_T(T) = \sqrt{\hbar D/k_B T}$, we obtained $\xi_T(T^*) = 170$ nm, which is comparable to L_ϕ . Thus, the suppression of ZBCP at higher temperatures than T^* was attributed to a dephasing effect due to thermal fluctuations, resulting in $\xi_T(T) < L_\phi$. We note that T^* is higher than the dephasing temperature estimated from the Thouless energy: $T_{\text{Th}} = eV^*/k_B = 2.6$ K. This underestimation of V^* can be caused by a finite background conductance at voltages below V_{gap} on the dI/dV vs. V curve resulting from a finite interfacial barrier at the N–S interfaces of the InAs NW sample.

When the magnetic field B was applied perpendicular to the substrate, the ZBCP was suppressed and eventually vanished at $B^* = 36$ mT, as shown in Figure 3a and 3b. Because the critical magnetic field B_C of the superconducting PbIn electrode [13] was found to be larger than 200 mT, the disappearance of the ZBCP is not caused by the magnetic-field-induced suppression of superconductivity in the PbIn electrode. Rather, it was attributed to broken time-reversal symmetry, which causes a phase shift between the electron and its retro-reflected hole during the reflectionless tunneling process. Because the total phase shift is given by [8] $\Delta\phi = 2\pi BA/\Phi_0$, where $\Phi_0 = h/2e$ is the magnetic flux quantum and A is the effective area enclosed by the superconductor and a loop formed by the trajectory of the scattered electron and retro-reflected hole, we obtained $A = 0.062 \mu\text{m}^2$ from $\Delta\phi(B^*) = 2\pi$. When the lateral width is approximated by the NW diameter, the effective length turned out to be $L_{\text{eff}} = 0.78 \mu\text{m}$, which is much longer than the channel length. The difference between L and L_{eff} can be explained by the London penetration depth (λ) of PbIn, which resulted in $\lambda = L_{\text{eff}} - L = 560$ nm. This value is comparable to $\lambda \sim 450$ nm in the

previous report [14].

In conclusion, we observed ZBCP in an InAs NW contacting PbIn superconducting electrodes. The temperature, bias voltage, and magnetic field dependencies of the ZBCP were consistent with the theoretical expectations of the phase-coherent electronic transport via reflectionless tunneling. The characteristic energy for observing the ZBCP was determined by the Thouless energy of the NW, while the phase coherence between the electron and its retro-reflected hole was preserved. Our experimental studies would provide clear criteria for discriminating between ZBCPs due to the Andreev reflection and due to Majorana fermions.

Acknowledgment

This work was supported by the “GIST-Caltech Research Collaboration Grant” funded by the GIST in 2017.

Figure Captions

Figure 1. (a) SEM image of the InAs NW device (**D1**) with the typical measurement configuration. The current bias I is applied between two PbIn electrodes (+I and -I) through the InAs NW, and the voltage V is monitored between the +V and -V electrodes. (b) Differential conductance G of sample **D2** with the back-gate voltage V_g at $T = 10$ K. V_g was applied to the Si substrate, and the source-drain bias voltage was $V_{SD} = 1$ mV.

Figure 2. (a) R vs. T plot obtained from sample **D1**. The superconducting transition temperature was $T_C = 7.3$ K. The red solid line represents the fitting result (see text). (b) Normalized conductance (G) as a function of V at $T = 2.4$ K. The characteristic voltage V^* for the ZBCP was about 0.22 mV, and the gap voltage V_{gap} was 2.3 mV. (c) Lock-in voltage (V_{ac})

dependence of the ZBCP at $T = 2.4$ K. From top to bottom, $V_{ac} = 3.9$ μ V (black), 11 μ V (red), 22 μ V (blue), 130 μ V (green), and 310 μ V (magenta). The curves are offset for clarity. (d) Temperature dependence of the ZBCP. From top to bottom, $T = 2.4$ K (black), 2.7 K (red), 3.0 K (blue), 3.3 K (green), and 3.6 K (magenta). The curves are offset for clarity.

Figure 3. (a) G vs. V curve with varying magnetic field at $T = 2.4$ K. From top to bottom, $B = 0$ mT (black), 14 mT (red), 25 mT (blue), 29 mT (green), and 34 mT (magenta). The curves are offset for clarity. (b) Zero-bias conductance as a function of the B field. B^* was about 36 mT, and B_C was about 280 mT.

Reference

- [1] Y.-J. Doh, J.A. van Dam, A.L. Roest, E.P.A.M. Bakkers, L.P. Kouwenhoven, S. De Franceschi, Tunable supercurrent through semiconductor nanowires, *Science*, 309 (2005) 272-275.
- [2] Y.-J. Doh, S. De Franceschi, E.P.A.M. Bakkers, L.P. Kouwenhoven, Andreev reflection versus Coulomb blockade in hybrid semiconductor nanowire devices, *Nano Lett.*, 8 (2008) 4098.
- [3] F. Giazotto, P. Spathis, S. Roddaro, S. Biswas, F. Taddei, M. Governale, L. Sorba, A Josephson quantum electron pump, *Nat. Phys.*, 7 (2011) 857-861.
- [4] L. Hofstetter, S. Csonka, J. Nygard, C. Schonenberger, Cooper pair splitter realized in a two-quantum-dot Y-junction, *Nature*, 461 (2009) 960-963.
- [5] G. de Lange, B. van Heck, A. Bruno, D.J. van Woerkom, A. Geresdi, S.R. Plissard, E.P.A.M. Bakkers, A.R. Akhmerov, L. DiCarlo, Realization of Microwave Quantum Circuits Using Hybrid Superconducting-Semiconducting Nanowire Josephson Elements, *Phys. Rev. Lett.*, 115 (2015) 127002.
- [6] T.W. Larsen, K.D. Petersson, F. Kuemmeth, T.S. Jespersen, P. Krogstrup, J. Nygård, C.M. Marcus, Semiconductor-Nanowire-Based Superconducting Qubit, *Phys. Rev. Lett.*, 115 (2015) 127001.
- [7] A. Das, Y. Ronen, Y. Most, Y. Oreg, M. Heiblum, H. Shtrikman, Zero-bias peaks and splitting in an Al-InAs nanowire topological superconductor as a signature of Majorana fermions, *Nat. Phys.*, 8 (2012) 887-895.
- [8] B.J. van Wees, P. Devries, P. Magnee, T.M. Klapwijk, Excess Conductance of Superconductor-Semiconductor Interfaces Due to Phase Conjugation between Electrons and Holes, *Phys. Rev. Lett.*, 69 (1992) 510-513.
- [9] A.F. Andreev, The Thermal Conductivity of the Intermediate State in Superconductors, *JETP Lett.*, 19 (1964) 1228-1231.
- [10] M. Popinciuc, V.E. Calado, X.L. Liu, A.R. Akhmerov, T.M. Klapwijk, L.M.K. Vandersypen, Zero-bias conductance peak and Josephson effect in graphene-NbTiN junctions, *Phys. Rev. B*, 85 (2012) 205404.
- [11] H.Y. Gunel, N. Borgwardt, I.E. Batov, H. Hardtdegen, K. Sladek, G. Panaitov, D. Grutzmacher, T. Schaperes, Crossover from Josephson Effect to Single Interface Andreev Reflection in Asymmetric Superconductor/Nanowire Junctions, *Nano Lett.*, 14 (2014) 4977-4981.
- [12] Y.M. Yang, X.Y. Peng, H.-S. Kim, T. Kim, S. Jeon, H.K. Kang, W. Choi, J.D. Song, Y.-J. Doh, D. Yu, Hot Carrier Trapping Induced Negative Photoconductance in InAs Nanowires toward Novel Nonvolatile Memory, *Nano Lett.*, 15 (2015) 5875-5882.
- [13] S.-I. Park, H.-S. Kim, J.S. Lee, Y.-J. Doh, Characterizing Pb-based superconducting thin films, *Progress in Superconductivity and Cryogenics*, 16 (2014) 36-39.
- [14] D. Jeong, J.-H. Choi, G.-H. Lee, S. Jo, Y.-J. Doh, H.-J. Lee, Observation of supercurrent in PbIn-graphene-PbIn Josephson junction, *Phys. Rev. B*, 83 (2011) 094503.
- [15] J. Yoo, C.-H. Lee, Y.-J. Doh, H.S. Jung, G.-C. Yi, Modulation doping in ZnO nanorods for electrical nanodevice applications, *Appl. Phys. Lett.*, 94 (2009) 223117.

- [16] G. Blonder, M. Tinkham, T. Klapwijk, Transition from metallic to tunneling regimes in superconducting microconstrictions: Excess current, charge imbalance, and supercurrent conversion, *Phys. Rev. B*, 25 (1982) 4515.
- [17] H.-S. Kim, B.-K. Kim, Y. Yang, X. Peng, S.-G. Lee, D. Yu, Y.-J. Doh, Gate-tunable superconducting quantum interference devices of PbS nanowires, *APEX*, 9 (2016) 023102.
- [18] Y.-J. Doh, A.L. Roest, E. Bakkers, S. De Franceschi, L.P. Kouwenhoven, Quantum Interference Effects in InAs Semiconductor Nanowires, *J. Korean Phys. Soc.*, 54 (2009) 135-139.
- [19] P.H.C. Magnee, N. van der Post, P.H.M. Kooistra, B.J. van Wees, T.M. Klapwijk, Enhanced conductance near zero voltage bias in mesoscopic superconductor-semiconductor junctions, *Phys. Rev. B*, 50 (1994) 4594.

Figure 1

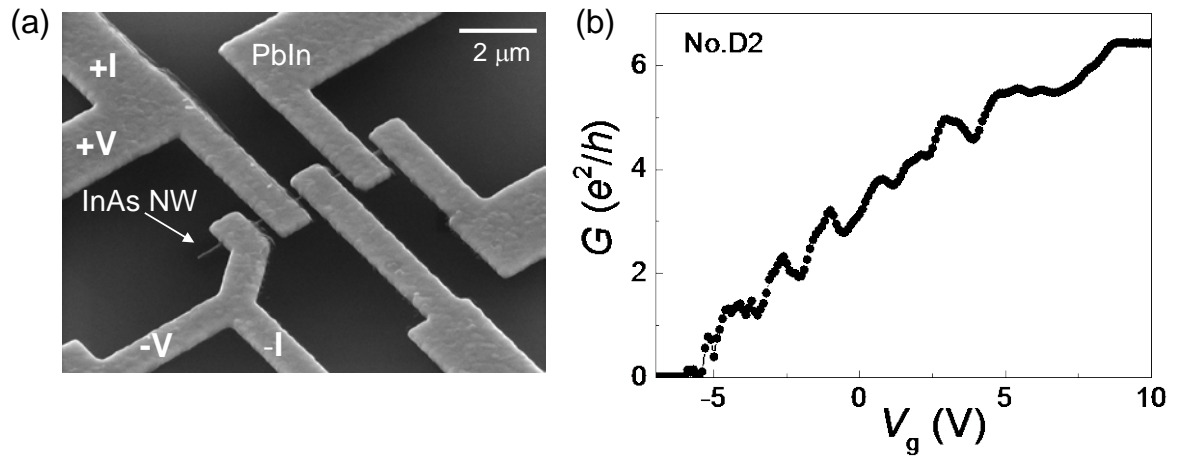


Figure 2

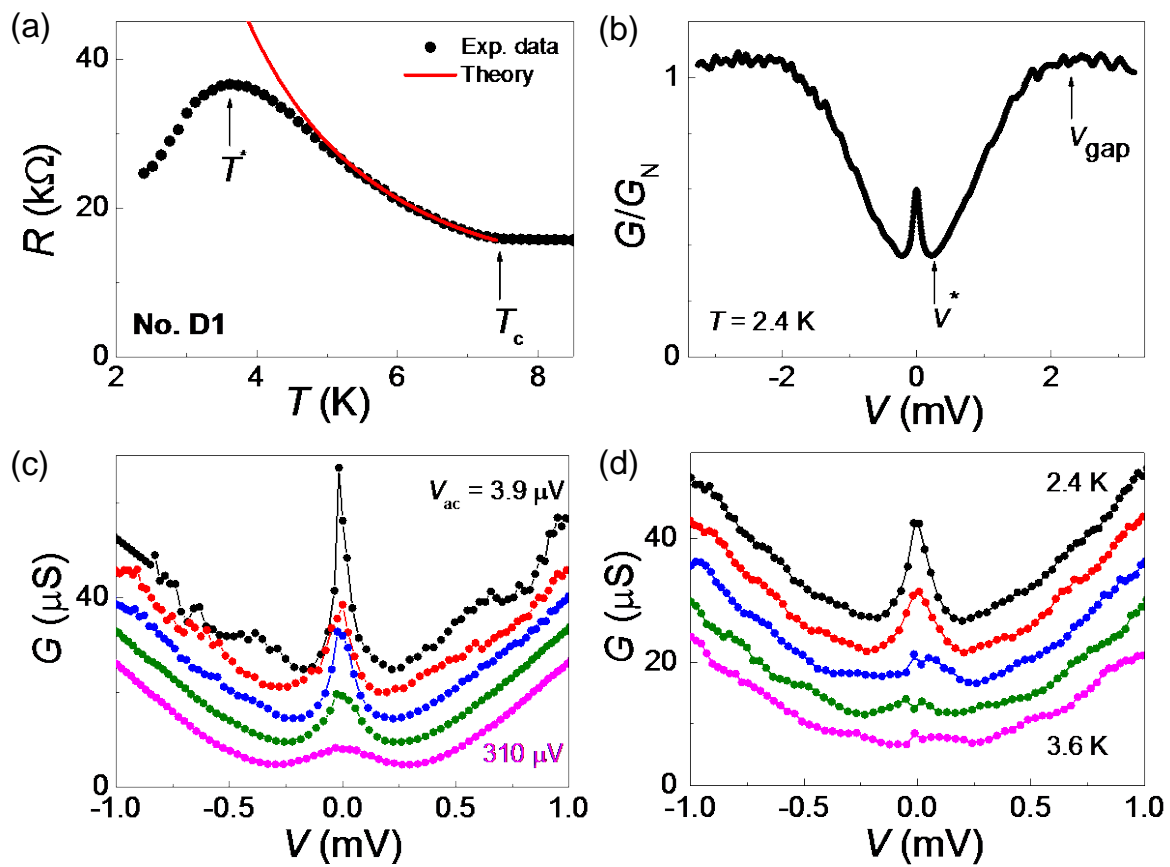


Figure 3

